A Combined Approach Based on Design of Experiments and Numerical Modelling for Mechanical Performance of 3D Printed Polylactic Acid/Carbon Fibre Composites

M. Lee and Y. Dong*

School of Civil and Mechanical Engineering, Curtin University

GPO Box U1987, WA 6845, Australia

* *Corresponding author (y.dong@curtin.edu.au)*

Keywords: *fused deposition modelling (FDM); composite materials; mechanical properties; design of experiments (DoEs); finite element analysis (FEA)*

1. Abstract

This paper compared mechanical properties of polylactic acid (PLA) and PLA/carbon fibre (CF) composites in Taguchi design of experiments (DoEs) to determine the effect of processing parameters such as layer thickness, infill density, raster angle and infill pattern on mechanical performance of 3D printed composite parts along with parametric optimisation. PLA yielded consistently higher tensile strength when compared with PLA-CF composites due to CF aggregation and poor filler-matrix interfacial bonding in such composites. The selection of PLA-CF composites proved to be advantageous over PLA for non-critical applications with the requirement of minimal elongation and deflection. Infill density was deemed the most significant factor to maximise tensile strength. In particular, increasing infill density resulted in more effective load distribution, thus improving interlayer bonding and decreasing void defects. When considering layer thickness, medium and high levels of 0.2 and 0.3 mm induced an optimal balance between maximising surface contract between layers and reducing total numbers of layers. It was also suggested infill pattern should be used with minimal infill gaps, and raster angle should be aligned parallel to primary loading direction for further optimisation of mechanical strength and elongation at break. 3D printed hinge models were set up using finite element analysis (FEA) to predict applied loads in good agreement with hinge testing data. The predicted stress distribution offers an insight into design modification to enhance more uniform stress distribution in both hinge leaves, and minimise the points of a major concern for critical mechanical failure.

2. Introduction

Fused deposition modelling (FDM) is one of the most popular additive manufacturing (AM) methods for manufacturing parts from polymer or composite materials by employing continuous thermoplastic filaments as raw materials. FDM consists of a liquefier head to melt these materials into a liquid state, which are then selectively deposited through a nozzle that traces the cross-sectional geometry of a part in a layer-by-layer manner in order to produce 3D parts directly from a CAD model. PLA, a popular biodegradable polymer derived from lactic acid, is amongst the most useful materials in AM, which is also deemed one of the widely employed matrix materials in fibre-reinforced composites due to its relatively low melting temperature and high processibility to achieve favourable outcomes with good biodegradability. As such, a wide range of fields including automotive, aerospace and medical industries rely on FDM to create design prototypes, functional parts and custom tooling. Among them, mechanical performance of additively manufactured parts is vital for part functionality and effective design testing. In particular, mechanical properties of additively manufactured parts can be enhanced by using filament materials with high mechanical strength via FDM, along with the optimisation of various processing parameters manipulated in AM processes [1]. Patadiya et al. [2] reported that the selection of build orientation greatly influenced mechanical properties of FDM printed parts with respect to strength, ductility and fracture patterns owing to different layer orientation in relation to the loading direction. Sandanamsamy et al. [3] suggested that the orientation of raster angle parallel to the loading direction induced the enhancement of tensile strength of 3D printed PLA due to the fracture of individual layers in comparison with the separation of adjacent raster layers. Nugroho et al. [4] found that flexural strength of additively manufactured PLA parts improved when increasing the layer thickness from 0.4 to 0.5 mm owing to stronger layer bonding and reduced ductility. Further, interlayer bonding was proven to induce strong impact on mechanical properties of additively manufactured parts. Tanveer et al. [5] evaluated the effects of infill density on FDM printed parts and reported that higher infill densities enhanced mechanical strength owing to improved interlayer bonding between consecutive layers. Nonetheless, lower infill densities created air gaps between layers, acting as crack propagators under tensile loads and absorbers in compressive loads. Akhoundi and Behravesh [6] compared various infill patterns of additively manufactured 3D parts, which suggested that high tensile and flexural strengths occurred in Hibert curve and concentric patterns with 100% infill density because of less voids.

With numerous processing parameters used in FDM, various methods [7] were employed to optimise and determine the contribution of selected parameters of interest. Taguchi method is one of most popular statistical analysis methods used in design of experiments (DoEs) with typical advantages ranging from the minimisation of total number of experiments, the reduction of production time and cost, the ability to optimise processing parameters, and identification of robust design solutions via signal to noise ratio (*S/N*) and analysis of variance (ANOVA) [8].

Additively manufactured PLA/CF composites were also under investigation in an effort to improve tensile properties of neat PLA. Maqsood and Rimašauskas [9] reported that PLA reinforced with continuous CFs showed a 460% increase in tensile strength compared to neat PLA and PLA/short CF composites. More importantly, poor interfacial bonding between short CFs and PLA matrices were also presented according to optical microscopy, along with air voids as typical defects in PLA/continuous CF composites. Similarly, Cao et al. [10] compared tensile properties of additively manufactured PLA and PLA composites reinforced with short CFs. However, tensile strength of PLA specimens was reduced from 54.51 to 49.41 MPa though an increase took place in both Young's modulus and elongation at break for PLA/CF composites (PLA-CF). The decline of tensile strength in PLA-CF may be ascribed to CF clustering effect and poor fibre-matrix interfacial bonding. Such studies highlight critical factors such as fibre length, fibre distribution and interfacial bonding to play an important part in enhancing mechanical properties of additively manufactured composite materials.

Current research focuses on mechanical measurement of additively manufactured standard testing specimens while testing non-standard customised parts remains limited in real applications. This is only exemplified by additively manufactured aerospace bracket, orthopaedic corset fastener and robotic components. This study aimed to evaluate the effect of complex processing parameters including layer thickness, infill density, infill pattern and raster angle, as well as material composition based on PLA and PLA-CF on tensile properties of additively manufactured composite parts via Taguchi method. Optimal condition also applied to the fabrication of additively manufactured hinge for advanced AM design and development.

3. Materials and Methods

3.1. Materials

PLA and PLA/CF composites used in this study were both based on polylactide (CAS9051-89-2) and the latter also contained 10 wt% chopped CFs. Corresponding filament materials (filament diameter: 1.75 mm) were directly purchased from Bilby 3D, NSW, Australia and Spectrum Filaments (Poland) respectively.

3.2. Printing Process

A Creality Ender 3 V3 SE printer (Shenzhen Creality 3D Technology Co., Ltd, China) was employed in this study. All CAD models were produced by SolidWorks and then directly imported into Creality Print software in STL files to set up various printing parameters, along with subsequent model slicing for 3D printing. Four key processing parameters, namely layer thickness, infill density, infill pattern and raster angle were selected for processing optimisation, along with three levels for each processing parameter to create an L_9 orthogonal array in Table 1. Raster angle here refers to the orientation of deposited infill lines known as rasters relative to x-axis of build platform (parallel to the front edge of the build plate) on our used 3D printer.

Table 1. Taguchi L_9 orthogonal array with different processing parameters and levels

Run	Layer Thickness (mm)	Infill Density (%)	Infill Pattern	Raster Angle
1	0.1	20	Triangles	0°
2	0.1	60	Grid	60°
3	0.1	99	Rectilinear	90°
4	0.2	20	Grid	90°
5	0.2	60	Rectilinear	0°
6	0.2	99	Triangles	60°
7	0.3	20	Rectilinear	60°
8	0.3	60	Triangles	90°
9	0.3	99	Grid	0°

3.3. Mechanical testing and microscopic analysis

Tensile tests were conducted using a Shimadzu Autograph AGS-X universal testing machine (UTM) with a 10 kN load cell. The experimental data was acquired using TRAPEZIUM-X software, which was subsequently processed in Microsoft Excel for a detailed analysis. Type I dog-bone testing specimens were employed at the crosshead speed of 5 mm/min according to ASTM D638 standard. Four specimens for each DoE run were printed and further tested to detect mechanical properties with test repeatability. The design of printed PLA and PLA-CF hinges was chosen in this study in non-standard tensile testing at the crosshead speed of 1mm/min on the same Shimadzu universal testing machine according to Figure 1. For microscopic analysis, Pro-MicroScan eyepiece camera (Oplenic Corporation, China) and BX51M microscope (Olympus, Japan) were utilised to analyse fractured morphology of all printed testing specimens in this study.

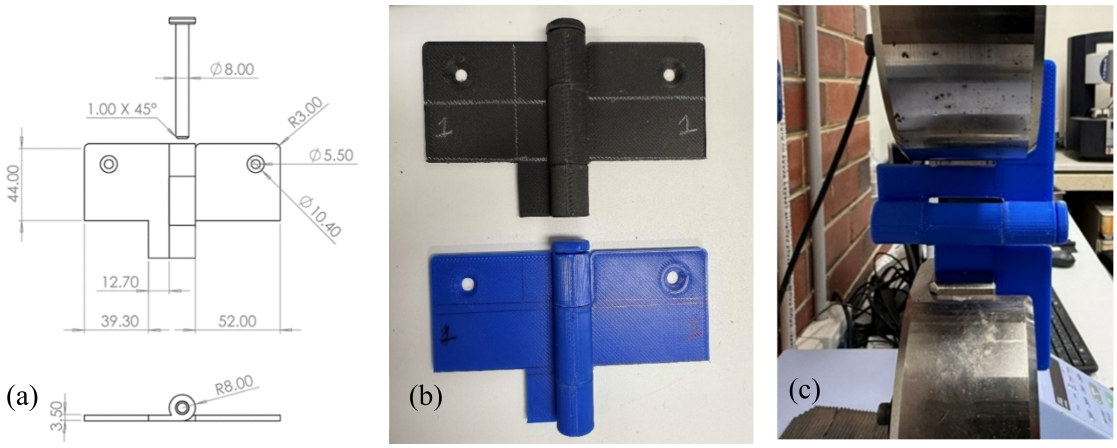

Figure 1. (a) hinge design sketch (all dimensions in mm), (b) PLA-CF (top) and PLA (bottom) and (c) hinge UTM mounting method

3.4. DoE response and Pareto ANOVA

The signal to noise ratio (*S/N*) was calculated for each individual DoE run using "the larger-the-better" criterion in order to maximise tensile and flexural strengths/strains as follows:

$$S/N = -10\,log\left(\frac{1}{n}\sum_{i=1}^{n}\frac{1}{y_i^2}\right) \quad (1)$$

where n is the number of samples and y_i is the response value in each run. Optimal factorial levels can be determined by calculating average *S/N* ratios at each level to produce main effect plots.

When using Pareto ANOVA, the sum of square difference is calculated using Equation 2:

$$S_B = (\Sigma B_1 - \Sigma B_2)^2 + (\Sigma B_1 - \Sigma B_3)^2 + (\Sigma B_3 - \Sigma B_2)^2 \quad (2)$$

where *B* represents one of the four selected processing parameters. Following the calculation of the sum of square difference, the contribution ratio of each processing parameter is then determined using Equation 3:

$$Contribution\ Ratio = \frac{S_B}{\Sigma S} \quad (3)$$

Once contribution ratios of all four processing parameters are calculated, a cumulative contribution of 90% is selected as the desired criterion to determining significant factors in DoE analysis.

4. Results and Discussion

4.1. Tensile properties

Tensile properties of PLA and PLA-CF are summarised in Table 2. Both PLA and PLA-CF had very similar ultimate tensile strengths despite being slightly higher for runs 1 to 3 in PLA-CF increasing by approximately 0.7 to 1.4 MPa, as opposed to 0.6 to 3.4 MPa increase for runs 4 to 9 in PLA. Accordingly, PLA consistently outperformed PLA-CF in ultimate tensile strength (UTS). However, the difference between these two materials lies in the elongation at break in which PLA could experience slightly high strain in range of 0.4-1.35% relative to those of PLA-CF though PLA is deemed a very brittle polymeric material. Moreover, higher stiffness became manifested for PLA-CF, increasing by approximately 0.6 to 1.1 GPa when compared with those of neat PLA.

Table 2. Data summary of tensile properties of PLA and PLA-CF in our DoE study

Run	Ultimate tensile strength (UTS) (MPa)		$(S/N)_{UTS}$ (dB)		Elongation at break ($\varepsilon_{t_{fracture}}$) (%)		$(S/N)_{\varepsilon_{t_{fracture}}}$ (dB)		Tensile modulus (GPa)	
	PLA	PLA-CF	PLA	PLA-CF	PLA	PLA-CF	PLA	PLA-CF	PLA	PLA-CF
1	29.1	30.5	29.6	29.7	2.4	1.8	7.9	5.1	1.8	2.8
2	34.0	35.4	30.8	30.9	2.9	1.9	8.8	5.2	1.9	3.0
3	40.6	41.3	32.7	32.4	2.8	2.1	9.3	5.8	2.3	3.5
4	35.6	35.6	31.2	30.7	2.6	2.0	8.5	5.2	2.1	3.0
5	40.2	38.9	32.1	31.7	2.8	2.0	10.0	6.5	2.3	3.3
6	41.1	38.9	32.0	31.8	2.3	1.9	8.2	5.7	2.5	3.3
7	34.7	31.3	30.4	30.0	3.2	2.2	9.8	7.0	2.0	2.7
8	37.1	34.6	31.4	30.8	3.3	1.9	10.4	6.1	2.2	2.9
9	40.2	39.6	32.3	32.0	2.8	2.1	9.8	6.1	2.4	3.3

There is a similar increasing trend in both ultimate tensile strength and tensile modulus for PLA and PLA-CF shown in Figures 2. Optimal processing parameter levels for the maximisation of ultimate tensile strength can be identified with the layer thickness of 0.2 mm, infill density of 99%, as well as a rectilinear infill pattern at the raster angle of 90°. Infill density was determined to be the most influential factor with significant contribution ratios of 71% and 81.21% for PLA and PLA-CF respectively, which is in good accordance with previous study indicating a dominant role of infill density to affect strength and stiffness, porosity, material stability, layer adhesion and material sintering [11]. The impact of layer thickness is less pronounced at 10.57% for PLA, followed by infill pattern and raster angle at 9.23% and 9.19%. In comparison, infill pattern indicates only contribution ratios of 9.23% and 8.70% for corresponding PLA and PLA-CF. When maximising elongation at break, Optimal condition took place with the layer thickness of 0.3 mm, infill density of 60% in a rectilinear infill pattern, along with negligible effect of raster angle for both PLA and PLA-CF. Layer thickness, infill pattern and infill density are considered as the most significant factors for PLA, while layer thickness and infill pattern are the highest contributors for PLA-CF instead. The optimal condition achieved at the infill density of 99% can be attributed to better interlayer bonding and significant reduction of voids as typical defects at a very high infill density level (i.e., almost a solid material sample).

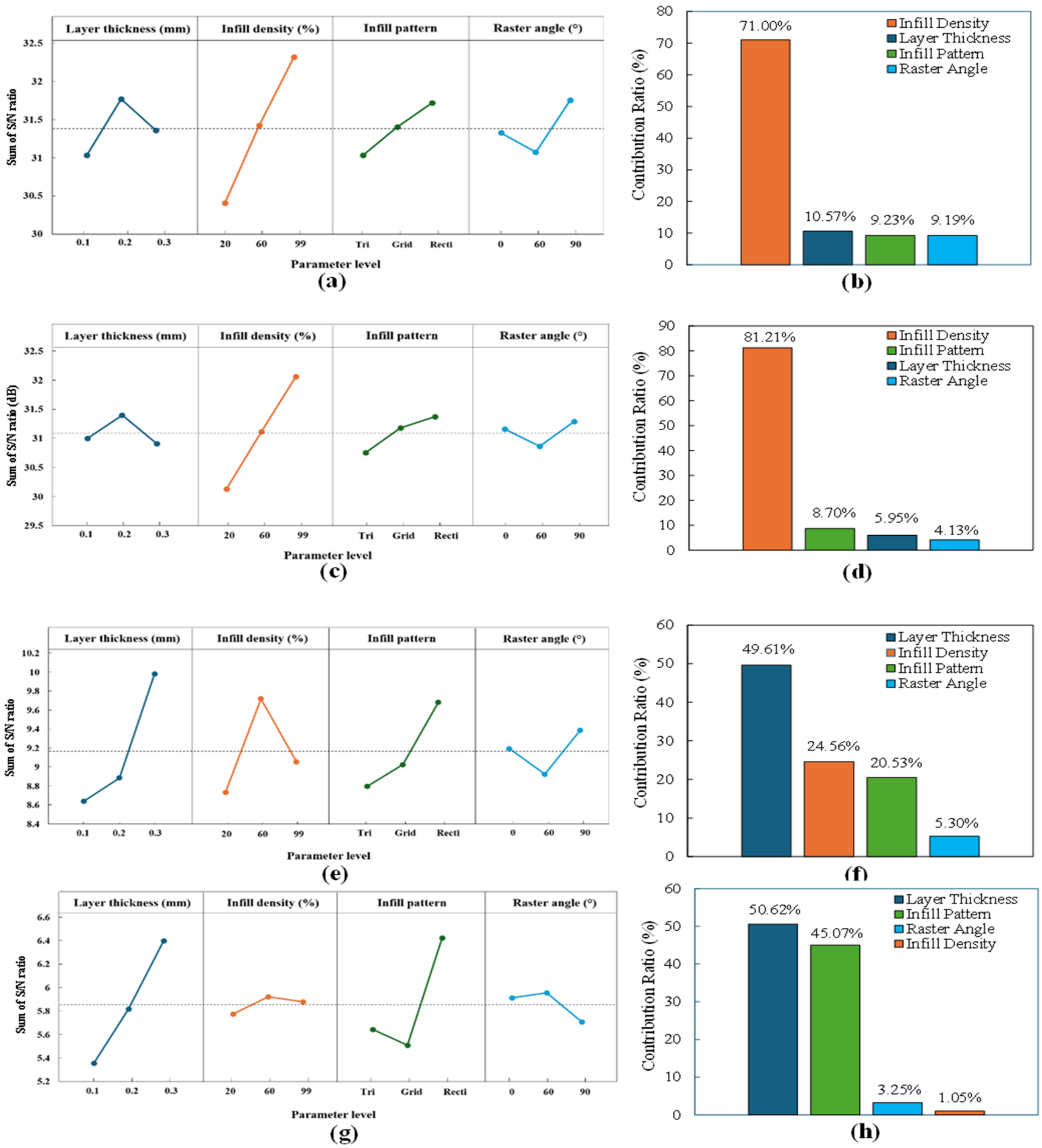

Figure 2. Main effect plots and contribution ratio charts to maximise ultimate tensile strength (a) and (b) for PLA, (c) and (d) for PLA-CF, as well as to maximise elongation at break (e) and (f) for PLA, and (g) and (h) for PLA-CF respectively.

4.2. Microstructural analysis

At the small layer thickness of 0.1 mm, surface contact between layers is supposed to be the greatest. However, in practice a lower layer thickness inevitably occurs, which means the requirement of a larger number of layers with the high possibility of poor interlayer bonding and voids as typical defects taking place in this study, as illustrated in Figures 3(a) and (b). On the contrary, higher layer thicknesses of 0.2 and 0.3 mm yield a lower number of layers, and thus induce less interlayer surface contact owing to much thicker layers built up according to Figures 3(c)-(f). Apparently, poor interlayer bonding and voids are most likely to be reduced with decreasing the total number of layers, which becomes more influential to optimise tensile properties instead of relying on lower layer thickness to maximise layer surface contact. This result also explains the reason why layer thickness of 0.3 mm and infill density of 60% are deemed the optimal condition to maximise elongation at break. In particular, there appeared to be high interlayer surface contact with the layer height of 0.2 mm and infill density of 99% leading to more compact and rigid structures, as evidenced by the increases in tensile modulus by 5.55% and 12.41% for PLA and PLC-CF when compared with those with the layer thickness of 0.3 mm. A similar trend of increasing tensile modulus by 20.78% and 15.02% for PLA and PLA-CF also became manifested relative to those with 60% infill density accordingly.

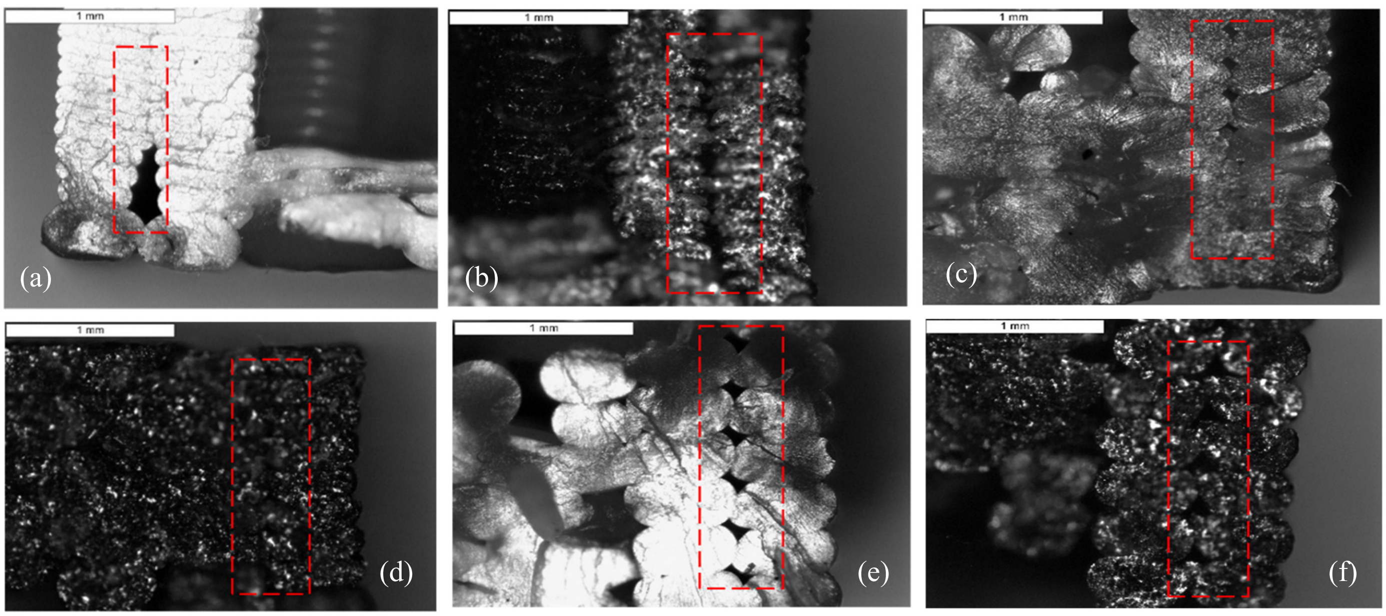

Figure 3. Optical micrographs of fractured tensile specimens of PLA (left) and PLA-CF (right) samples (a) and (b) for run 1 with 0.1 mm layer thickness, (c) and (d) for run 5 with 0.2 mm layer thickness, (e) and (f) for run 7 with 0.3 mm layer thickness.

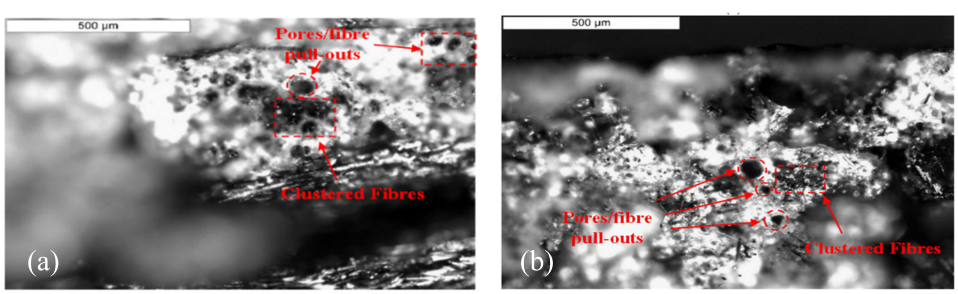

Figure 4. Optical micrographs of fractured tensile specimens of PLA-CF (a) run 7 and (b) run 5 tensile testing samples.

As for the declining phenomenon of ultimate tensile strength for PLA-CF relative to PLA, it could be clearly seen in Figures 4 that chopped carbon fibres in a random distribution tended to be in form of fibre clustering, potentially causing poor interfacial bonding between carbon fibres and PLA matrices, along with typical fibre pull-out and substantial amounts of pores within internal structures. Hence, this phenomenon inevitably induced more stress concentration sites and poor load transfer leading to weak load boarding capacity, as indicated by lower ultimate tensile strength identified in PLA-CF relative to that of neat PLA. This result coincides with previous studies [10, 12, 13] in which clustering of carbon fibres and poor fibre-matric bonding were proven to be major contributors in decreasing the tensile strength of PLA composites.

4.3. Numerical prediction using FEA

In order to validate experimental results in additively manufactured hinge tests, a finite element analysis (FEA) using ANSYS was conducted solely for elastic material behaviour. Boundary conditions of FEA model were set up in such a way that one end of the hinge was fixed while another end underwent uniaxial displacement accordingly. Finally, the reaction force at the fixed end were compared with corresponding data in hinge tests. Among material parameters used in FEA, the densities were obtained from material manufacturing data sheets, and Poisson's ratio of PLA was estimated based on previous FEA work [14], while Poisson's ratio of PLA-CF was assumed to be the same due to using a low CF content of only 10 wt% for simplicity. Young's modulus for PLA and PLA-CF was also obtained from tensile modulus data in this study.

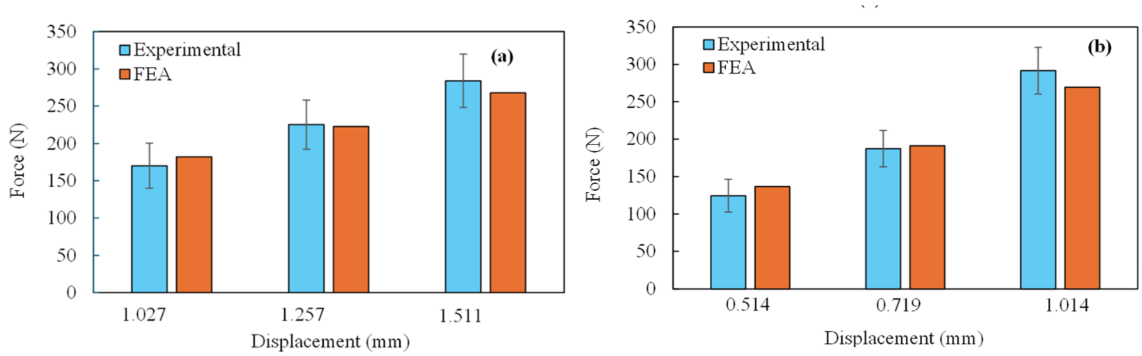

Figure 5. Comparison of experimental and numerically predicted forces: (a) PLA and (b) PLA-CF

Predicted results and experimental data were compared with respect to applied force shown in Figure 5 for PLA and PLA-CF respectively. Predicted forces are in reasonably good agreement with experimental data considering the use of some estimated material parameters and ideal conditions set up in FEA models. The difference between experimental and FEA forces became more evident since the hinges encountered the transition from linearly elastic behaviour to non-linear plastic behaviour beyond the deflections of 1.5 and 1 mm for PLA and PLA-CF respectively. Furthermore, FEA models overestimated the forces at low displacements of approximately 0.6 and 0.2 mm or less for PLA and PLA-CF accordingly, which may be related to small clearances between the pins and internal surfaces of hinged knuckles for real hinges in experiments. Nonetheless, this phenomenon is not present in FEA models. The stress distribution of FEA model illustrated in Figure 6 offers very useful insight into critical areas of the hinge towards mechanical failure. As depicted in Figure 20a, section B underwent a substantial area of high stress with a particular stress concentration region located at the right corner on the top surface of the hinge leaf. This is expected since stress concentration often happens at sharp corners, and this becomes the particular area where real hinges fractured in experiments. Accordingly, FEA hinge models support experimental data, which suggests that further iterations of hinges consist of design modification with respect to the number of knuckles to enhance a more uniform stress distribution in both hinge leaves and minimise the points of a major concern for critical mechanical failure.

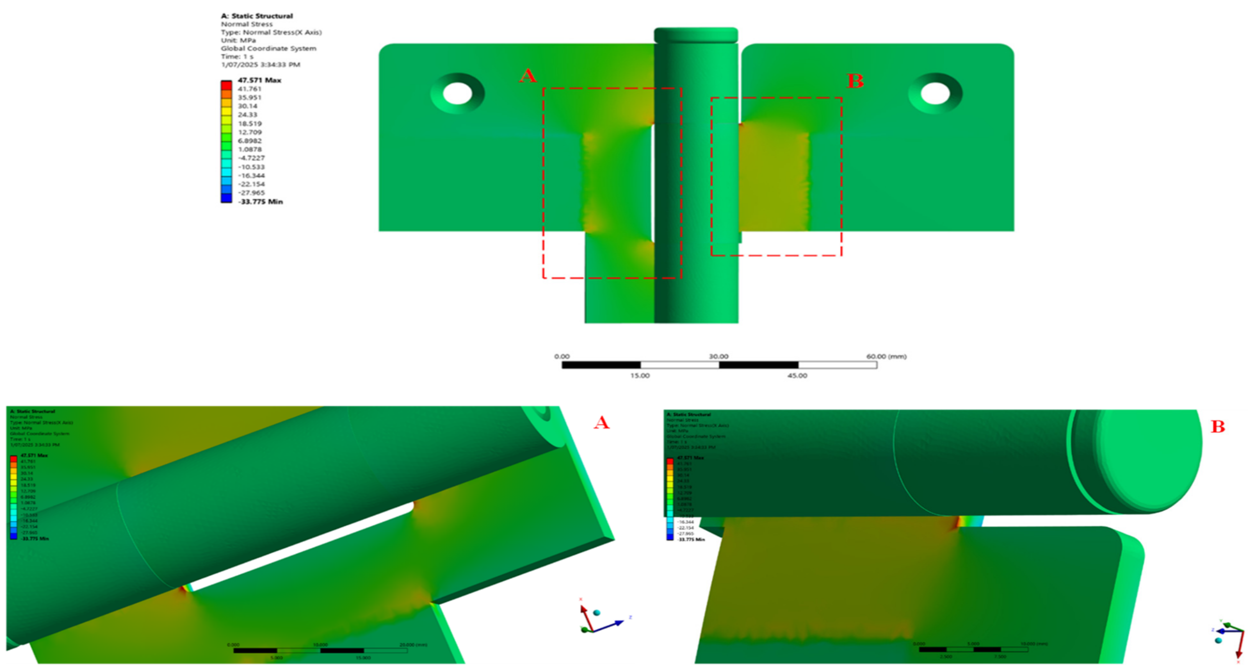

Figure 6. Stress distribution of PLA hinge with an applied displacement of 0.1207 mm

5. Conclusions

This study investigated the effects of layer thickness, infill density, infill pattern and raster angle, as well as material selection on tensile properties of additively manufactured mechanical testing samples and mechanical hinges for a real application. Ultimate tensile strengths of PLA and PLA-CF were very similar despite predominantly higher strength levels for PLA in range of 0.6-3.4 MPa. Better mechanical performance of PLA could arise from clustering effect of carbon fibres and poor interfacial bonding in PLA-CF. PLA is still a preferred material for functional parts and custom tooling in view of mechanical performance. Infill density was determined to be the most significant factor to maximise tensile strength. As for tensile strength, infill density made a major contribution ratios of 71.0% and 81.21% for PLA and PLA-CF respectively. The infill density of 99% was the optimal level mainly because high infill density induced better interlay bonding with significantly reduced voids and pores, along with a more uniform load distribution with additional solid materials to fill within internal structures. Among other processing parameters, layer thickness was identified to be optimal at 0.2 mm when maximising tensile strength alone. Overall, a good balance is vital between thinner layers to enhance layer surface contacts and thicker layers for reducing total number of layers used in additive manufacturing with minimal voids and porous structures. Predicted forces and stress distribution offers an effective numerical approach to be in good comparison with experimental results with a linearly elastic behaviour.

6. References

[1] D. Syrlybayev, B. Zharylkassyn, A. Seisekulova, M. Akhmetov and D. Talamona. "Optimisation of strength properties of FDM printed parts-A critical review". *Polymers*, Vol. 13, No. 10, 1587, 2021.

[2] N. H. Patadiya, H. K. Dave, S. R. Rajpurohit, M. S. Shunmugam and M. Kanthababu. "Effect of build orientation on mechanical strength of FDM printed PLA". In *Advances in Additive Manufacturing and Joining*, Springer, Singapore, pp 301-307, 2019.

[3] L. Sandanamsamy, J. Mogan, K. Rajan, W. S. W. Harun, I. Ishak, F. R. M. Romlay, M. Samykano and K. Kadirgama. "Effect of process parameter on tensile properties of FDM printed PLA". *Materials Today Proceedings*, Vol. 109, pp 1-6, 2024.

[4] A. Nugroho, R. Ardiansyah, L. Rusita and I. L. Larasati. "Effect of layer thickness on flexural properties of PLA (polylactic acid) by 3D printing". *Journal of Physics: Conference Series*, Vol. 1130, 012017, 2018.

[5] Md. Qamar Tanveer, G. Mishra, S. Mishra and R. Sharma. "Effect of infill pattern and infill density on mechanical behaviour of FDM 3D printed Parts-a current review". *Materials Today Proceedings*, Vol. 62, pp 100-108, 2022.

[6] B. Akhoundi and A. H. Behravesh. "Effect of filling pattern on the tensile and flexural mechanical properties of FDM 3D printed products". *Experimental Mechanics*, Vol. 59, pp 883-897, 2019.

[7] K. Rooney, Y. Dong, A. K. Basak and A. Pramanik. "Prediction of mechanical properties of 3D printed particle-reinforced resin composites". *Journal of Composite Science*, Vol. 8, No. 10, 416, 2024.

[8] N. Maguluri, G. Suresh and K.V. Rao. "Assessing the effect of FDM processing parameters on mechanical properties of PLA parts using Taguchi method". *Journal of Thermoplastic Composite Materials*, Vol. 36, No.4. pp1472-1488, 2023.

[9] N. Maqsood and M. Rimašauskas. "Characterization of carbon fiber reinforced PLA composites manufactured by fused deposition modelling". *Composites Part C: Open Access*. Vol. 4, 100112, 2021.

[10] M. Cao, T. Cui, Y. Yue, C. Li, X. Guo, X. Jia and B. Wang. "Investigation of carbon fiber on the tensile property of FDM-produced PLA specimen". *Polymers* Vol. 14, 5230, 2022.

[11] J. J. Fekiač, L. Kakošová, M. Krbata, M. Kohutiar, M. Eckert, Z. Studeny and A. Dubec. "Influence of infill geometry and density on the mechanical properties of 3D-printed polylactic acid structures". *Journal of Manufacturing and Materials Processing*, vol. 9, 134, 2025.

[12] S. Krishnakumar and T. Senthilvelan. "Characterization of PLA-CF composites fabricated by fused filament fabrication technique". *Transactions of the Indian Institute of Metals,* vol. 75, pp 2607-2616, 2022.

[13] M. Subramaniyan, S. Karuppan, A. Appusamy and N. Pitchandi. "Sandwich printing of PLA and carbon fiber reinforced-PLA for enhancing tensile and impact strength of additive manufactured parts". *Journal of Manufacturing Processes*, Vol. 137, pp 425-436, 2025.

[14] F. Aldosari, M. A. A.Khan, M. Asad and F. Djavanroodi. "Finite element analysis of polylactic acid (PLA) under tensile and compressive loading". *Journal of Physics: Conference Series*, Vol. 2468, 012094, 2023, *2468*.